Article

Not peer-reviewed version

# Adsorption of Chromium (VI) from Synthetic and Real Tannery Wastewater: Using Natural and Commercial Adsorbents

Destaw Sitotaw , Tesfaye Ababu , Andualem Mekonnen * , Tadesse Alemu

Posted Date: 31 March 2026

doi: 10.20944/preprints202603.2409.v1

Keywords: adsorption; chromium (VI); tannery wastewater; synthetic water

*Article*

# Adsorption of Chromium (VI) from Synthetic and Real Tannery Wastewater: Using Natural and Commercial Adsorbents

**Destaw Sitotaw [1], Tesfaye Ababua [2], Andualem Mekonnen [3,*] and Tadesse Alemu [3]**

[1] Ethiopian Conformity Assessment Enterprise, P.O. Box 11145, Addis Ababa, Ethiopia
[2] Ethiopian Biodiversity Institute, P.O. Box 30726, Addis Ababa, Ethiopia
[3] Pollution and sanitation stream, Center for Environmental Science, College of Natural and Computational Sciences, Addis Ababa University, P.O Box 1176, Addis Ababa, Ethiopia
* Correspondence: andumk21@gmail.com

**Abstract**

Chromium is one of the most prevalent toxic heavy metals in the environment and is known to cause cancer, and cellular damage. Various treatments can effectively remove Chromium ion from wastewater. However, majority of those methods are not environmentally friendly. Here, we investigated the efficacy of stem cactus activated carbon (SCAC) and commercial activated carbons (CAC) to remove hexavalent chromium from synthetic and real wastewater. In this study, the stem cactus adsorbent was thoroughly characterized. The effect of initial concentration of Cr (VI), contact time, adsorbent dose, shaking speed, and pH on the adsorption process were examined using Micro Plasma Atomic Emission Spectroscopy and UV-Vis Spectroscopy. The data were analyzed using R-software (version 4.4.3 (2025-02-28)) and Origin (2022). The trends in removal efficiency were examined descriptively using line graph. The adsorption equilibrium isotherms and kinetics models were fitted to the data to evaluate the biosorption mechanisms and compare the sorption capabilities of the two biosorbents (SAC and CAC). Under optimal conditions (0.15g SCAC, pH 2, contact time 60 min, shaking speed 200rpm, and an initial Cr (VI) concentration of 6mg/L), Cr (VI) removal efficiencies reached 98.4% and 99.2% from real and synthetic wastewaters, respectively. The adsorption data fitted both the Langmuir and Freundlich isotherm models, suggesting mixed homogenous and heterogenous surface characteristics on the adsorbent. The adsorption process is an endothermic process and respects the pseudo second order kinetics model. The present study suggests that plant-based adsorbents represent an effective alternative for Cr (VI) ion removal.

**Keywords:** adsorption; chromium (VI); tannery wastewater; synthetic water

---

## 1. Introduction

Chromium is one of the most prevalent toxic heavy metals in the environment and is frequently detected in industrial settings. This transition heavy metal are found in the metallic (Cr(0)), trivalent (Cr(III)), and hexavalent (Cr(VI)) states (DesMarias & Costa, 2019). Trivalent Chromium is prevalent in the rocks and soils, and is readily absorbed by plants, and enter into the food chain when animals and humans consume these plants (Uddin et al., 2007). Chromium ion pollution is a significant environmental issue because it causes a serious health effects in human and animals (Edo et al., 2024). Exposure to hexavalent Chromium can cause health problems, such as cancer, and cellular damage (DesMarias & Costa, 2019). In humans, Cr ion exposure can disrupt the normal functioning of the kidneys, heart, muscles, liver, central nervous system and other sensitive organs (Mane et al., 2011; Derbe & Yilma, 2015). Furthermore, it negatively impacts plant physiology by interfering with the process of photosynthesis (Pragathiswaran et al., 2013)). Industrial processes mainly tannery industry and dye, use chromium and are the major contributors to environmental pollution through the

 doi:10.20944/preprints202603.2409.v1



discharge of their untreated wastewater (Alfarra et al., 2014). Animals and plants are exposed to anthropogenic released of Chromium through inhalation of contaminated air and ingestion drinking water (Vimercati et al., 2017).

Various approaches existed in the literature can effectively remove Chromium from wastewater, even at high concentration levels(Islam et al., 2023). Traditional methods are mainly focused on removing and re-using of Chromium (Mohammadi et al., 2009). The conventional methods that have been extensively applied in Chromium removal are: solvent extraction, precipitation, chemical reduction, electrochemical treatment, membrane filtration, flotation and ion exchanges(Eghonghon et al., 2021). Of these flocculation and membrane filtrations are frequently applied in industries(Islam et al., 2023). However, majority of those methods are chemical-based, selective, extensive, needs sophisticated materials, and even poses another environmental problem. These issues necessitate to find environmentally friendly, fast, cheap, efficient and safe technologies as curative methods to remove hexavalent trivalent Chromium using locally available biosorbents(Islam et al., 2023; Kumar et al., 2025). To this end an adsorption approach have been developed to remove heavy metals from wastewater through their accumulation on the surface of an adsorbent. In the adsorption/sorption technique, tea waste peel, rice husk, banana fiber, sawdust, barley bran, eucalyptus sheathiana bark, and rice straw have been commonly used (Gupta et al., 2015). However, the use of stem cactus as biosorbent to remove hexavalent Chromium from wastewater has not been yet studied. The main objective of this study was to investigate the hexavalent Chromium removal efficiency of activated carbon derived from Cactus stem and commercial activated carbon as an adsorbent from synthetic and rail tannery wastewater.

## 2. Materials and Methods

*a. Materials*

i. Chemicals and Reagents

All reagents and chemicals used in this research were of analytical grade, and which were provided by the Ethiopian conformity assessment enterprise. The main reagents were, $K_2Cr_2O_7$ (purity≥99.9%) for oxidation-reduction processes, $H_2SO_4$ (purity ≥98%) to adjust the pH of the wastewater, NaOH (purity≥99%) for acid neutralization and pH adjustment, $KMnO_4$ (purity≥99%) as strong oxidizing agent, $NH_4OH$ (purity≥30%) for pH adjustment and , and 1,5, diphenyl carbazide ($C_{13}H_{14}N_4O$) (purity ≥99.9%) used as a colorimetric indicator, the products of Loba chemie industries were used for all calibration and batch investigation.

ii. Preparation of Biosorbent Materials

Fresh stem cactus was collected from Addis Ababa university compounds, Addis Ababa, Ethiopia. The stem cactus was properly washed, and rinsed with distilled water, and then cut in to strips of 1cm and sun-dried for two weeks, and then placing in the air and oven-dried for 24 hours at 105° C. The dried stem cactus was completely mixed with 45% (w/w) $H_3PO_4$ in a 2:1 ratio. The mixture was impregnated, and the stem cactus was left to soak overnight. $H_3PO_4$ is used as activation agent in the production of activated carbon. Furthermore, it has a greater impregnation ratio, which causes an excessive interaction between $H_3PO_4$ and carbon. To avoid extensive blockage of pores, a medium of impregnation ratio was used.

The sample was impregnated, and carbonized in the air electric oven, and then incinerated at 450 °C for 60 minutes, and carefully sealed with aluminum foil to prevent tar forming with ambient oxygen and cooled at ambient temperatures in in the presence of silica gel desiccators. The temperatures and time of durations were one hour and 450 °C, respectively to prevent pore formation. Then, the carbon was ground and sieved through 0.425mm pore size to produce a homogenous and delicate surface powder.

Preprints.org (www.preprints.org) | NOT PEER-REVIEWED | Posted: 31 March 2026 doi:10.20944/preprints202603.2409.v1



After the activator (phosphoric acid) removed from the carbonization products by double distillation water, the powder was dried for 24 hours at 110 °C, and then labelled and kept in tightly sealed sample vials in order to prevent moisture absorption, which is ready to use in adsorption experiment and FTIR measurements.

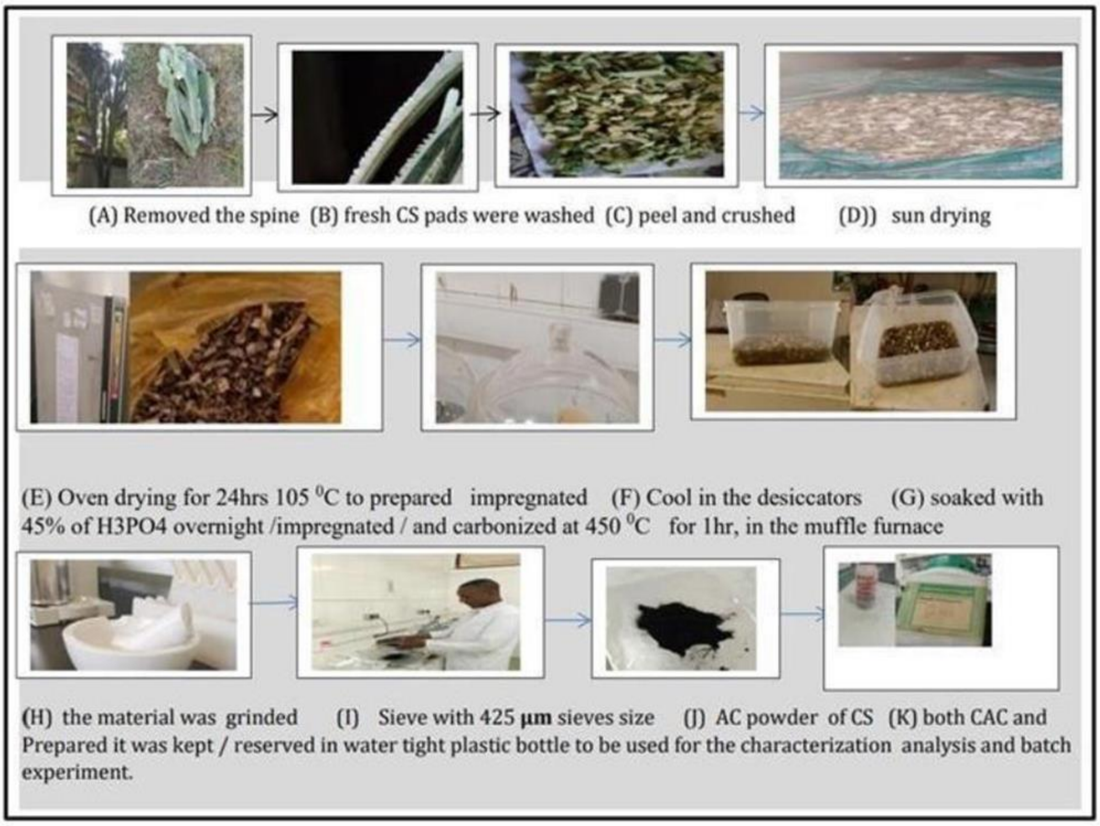


**Figure 1.** Flow chart showing preparation of activated carbon derived from stem cactus.

*b Methods*

iii. Adsorbent Characterization

To determine the moisture content of the activated carbon, one gram of the activated carbon powder was placed into the crucible, and oven-dried the contents at 110 °C for one hour, and then cooled at room temperatures in a desiccator. Then the moisture content of the activated carbon was determined using the AOAC (2000) formula:

$$\mathrm{MC} = \frac{(\mathrm{M1}+\mathrm{M2})-\mathrm{M3}}{\mathrm{M2}} * 100 \ldots\ldots\ldots\ldots\ldots 1$$

Where, MC= moisture content in %, by mass M 1 = mass of dish in gram, M2=mass of test portion (activated carbon) in gram and M3 = weight of residue and dish in gram after drying at 110ºC.

The ash content of the biosorbent was determined by measuring 1 g of cactus stem powder on a pre-weighed crucible. The content was placed in a furnace and ignited at 500 °C for an hour, until white grey residue formed. The crucible was transferred to a desiccator and weighed. Then the ash content (%) was determined using the AOAC (2000) formula:

$$Ash\ content(\%) = \frac{W2-W1}{MS} * 100 \ldots\ldots\ldots 2$$

Where: M2= is weight of the ash in gram, M1= the empty crucible in gram and MS= is original weight of the powder cactus sample.

To determine the volatile matter of the biosorbent, three grams of the air-dried sample of the biosorbent were placed in the pre-weighed crucible, and then heated in muffle furnace at 600 °C for 15 minutes. Then after, the crucible was removed from the oven and cool in the desiccators for 20 minutes before being measured. The crucible was then cooled and re-weighed, and the weight loss because of the release of the volatile matter. The volatile matter (%) was determined according to the standards of AOAC ( 2000) formula:

$$VM(\%) = \frac{M2 - M1}{M0} * 100 \ldots\ldots\ldots\ldots\ldots\ldots\ldots 3$$

Where: MV (%) is volatile matter in percent, M2= is weight of the ash in gram, M1= the empty crucible in gram and M0= is original weight of the powder cactus sample.

The fixed carbon content was determined after the moisture content, ash content and the volatile matter removed. The remaining carbon portion was determined using the following formula (Racero-Galaraga et al., 2024):

$$\mathrm{FC}(\%) = 100 - (\mathrm{MC} + \mathrm{VM} + \mathrm{AC}) \ldots\ldots\ldots\ldots\ldots 4$$

Where: FC is fixed carbon, Mc is the moisture content, AC is the ash content of activated carton, and VM is the volatile matter.

To determine the bulk density of the cactus stem biosorbent, a known mass of the activated carbon cactus stem was poured in a pre-weighed graduated measuring cylinder (250 ml), and the mass of the content was measured, and the volume of the sample was then recorded from the measuring cylinder (Illingworth et al., 2012). The Bulk density was calculated according to AOAC (2000):

$$\rho\mathrm{b}\left(\frac{\mathrm{g}}{\mathrm{mL}}\right) = \frac{\mathrm{MS} - \mathrm{Mc}}{\mathrm{Vc}} \ldots\ldots\ldots\ldots\ldots\ldots\ldots\ldots\ldots\ldots 5$$

Where: ϱb is bulk density, MS= mass in gram of the cactus stem biosorbent, Mc= mass in gram of measuring cylinder Vc =volume in ml of measuring cylinder (250ml).

The pH at point of zero charge of the adsorbent was determined using salt-method. Which means that the pH values of the surface charge became zero (Preočanin & Kallay, 2006). Ten 50 mL Conical flasks were equipped, each holding a 40 ml of 0.1M $NaNO_3$. The initial pH of the suspensions was maintained from 1 to 11 using 0.1M acid (HCl), and the pH values were evaluated using a calibrated pH meter. Then the contents were stirred over night at ambient temperatures and at 200 rpm. After these equilibrations, the final pH of each suspension was determined, and the pH change was computed. Change in pH versus initial pH was plotted, and the point at which change in pH equals to zero was used as the point of zero charge.

The FTIR analysis was determined using FTIR transmission spectra (Duran-valle, 1999). A known amount of oven-dried sample powder was placed on the FTIR sample holder, the spectra were recorded using an FTIR spectrometer in the range of 4000- 550cm$^{-1}$, where the absorption peaks correlated to the vibrational frequencies of the chemical bonds present in the cactus stem biosorbent.

The molecular arrangement (crystalline structure) of the adsorbent (Cactus stem) was analyzed through an X-ray diffraction analysis. The oven-dried, grounded, and mounted sample was analyzed using X-ray diffractometer via Cu K$\alpha$ radiation (at $\lambda$ = 1.5406 Å). The scans were documented between 5–80° (2θ), at 0.02° step size. The different diffraction peaks were identified using the ICDD database, and the crystallite size was determined using the Scherrer equation after correcting FWHM values for instrumental broadening. If the materials are crystalline, they will have well-defined peaks. Other ways, they displayed a hollow instead of well-peaked area (Reza & Ahmaruzzaman, 2015).

The surface appearance and fundamental physical characteristics of the stem cactus adsorbent was examined using scanning electron microscope. The dried, and finely ground cactus stem was coated a material that encourages conductivity. The surface texture, and particle structure were observed at a various observation, and an accelerating voltage of 5–20 kV (El-araby et al., 2017).

iv Determination of Chromium (VI) by Using Colorimetric Methods

Removals of reducing factors/agents in the extraction reagents by 2% NaOH

Reducing agents present in the reagents were removed using APHA (1926) by thoroughly mixing 2 ml of 0.1% KMnO4 solutions, and 2% NaOH solution in the reaction flask, and left for some minutes. The solution was then exposed, and 0.1% KMnO4 was added dropwise with gently mixing until lightly pink color observed.

Removal of reducing agent by 6N H2SO4

a solution of 0.75 ml KMnO4 (0.1%) was added to the flask containing 6N $H_2SO_4$ by gently pipetting, and then the contents were thoroughly mixed. After a short period of time, the solution was left to settle and then KMnO4 was added dropwise with gently mixing until a light pink color was observed (Clesceri et al., 1998; Kebede, 2013).

v. Preparation of Stock Solution

The hexavalent Chromium metal (1000mg/L) stock solution of was prepared by dissolving 2.83g of analytical reagent grade potassium dichromate ($K_2Cr_2O_7$) in a distilled water, and the volume was made up to 1000ml (Emirie, 2015).

vi. Preparation of Standard Curve for Cr (VI)

The standard solution for MP-AES and UV-vis calibration was prepared by adding from 1000mg/L of Chromium metals in to the solution. A calibration curve was produced using seven working standards generated by serial dilution of intermediate stranded (100mg/L Cr (VI)) solution. 1ml (10ppm) chromium standard solution was added into 100 ml of volumetric flask, and diluted with distilled water until the calibration mark achieved, then stoppered and gently mixed. Then after, the seven series of a 100 ml flasks series were each filled with 25 ml of this solution, which had formerly been treated through diluted KMnO4 solutions. To eliminate the carbon dioxide gas, each flask was filled with 0,0.5,1, 2, 4, 6, and10 ml Cr (VI) standard working solutions, and 7.8 mL in the 6N $H_2SO_4$ extracted solutions. 2 mL of diphenyl carbazide solution was added to dilute the content to the appropriate level. The flasks were sealed, and mix by turning the flasks upside down for many times, and then leave the samples for 15minutes until the full color observed. After calibrating the instrument, the absorbance of each sample was recorded in a1cm cuvette at a wave length of 540 nm was recorded, and then a calibration curve was prepared by plotting a linear graph of absorbance Vs mg $Cr^{+6}$ /50 ml (Clesceri et al., 1998; Kebede, 2013).

Preparation of synthetic hexavalent Chromium solution

To create the appropriate experimental solutions of 50 ml Cr (VI) with different initial concentrations and temperatures from 2 to 10 mg/L and 25 to 25 °C, respectively, different volumes of solution were diluted by water. Differential pH, dosage of stem cactus powder, duration of contact time, and speed of stirring, were between 2-7, 0.075-1.0g, 30-150min, and 50- 200 rpm, respectively.

vii. Batch Adsorption Experiment

In a batch adsorption experiment, numerous solutions and volumes were diluted for the necessary batch experiments solution (Figure 2).

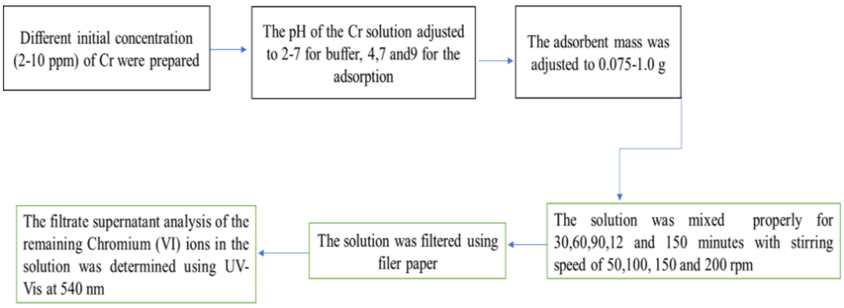

**Figure 2.** Experimental set up for the determination of optimum pH, Co, contact time, stirring speed, and adsorbent dose.

vii Experimental Methods for Real Wastewater Digestion and Oxidation

The amount of Cr (VI) values was determined using sample digestion and extraction methods. 100 mL of Chromium waste was added into a beaker containing a few boiling chips and 5 mL of $HNO_3$ (conc.). Prior to precipitation, the contents were heated to boiling, and allowed to evaporate until the volume reached to 20ml. Then, 5 ml of $HNO_3$ (conc.) was added to the final volume of 20 mL, the solution was cooled, and the whole mixture was filtered in 100 mL volumetric flask until a clear solution was observed, indicating complete digestion. As a follow-up, oxidization of Cr (III) was carried out by adding a few drops of Methyl orange indicator into a 125 ml flask containing the digested and the filtrate samples. Subsequently, ammonium hydroxide (conc) was added dropwise to the solution until a yellow color was observed, after which H2SO4 ($1^{+1}$) was added dropwise until the color change observed, and the volume was adjusted to around 40 mL and the contents were progressively heated and brought to a boil. Then, 2 mL of $KMnO_4$ solution were added to the contents until the color faded, after which two additional drops of $KMnO_4$ were added to produce a red color within five minutes of boiling the content. 1 mL of sodium azid (NaN3) indicator was added to the solution, which was then heated for 1 minutes followed by the further addition of 1 mL, and the contents were heated to boil for 1 minute until the color completely disappeared, and then the solution was subjected to cool. Finally, the resultant solution was tested using PM- AES determine Cr (VI)) ions.

**Figure 8.** MP-AES (Agilent Technologies,) Real Waste Water analysis.

The adsorption efficacy of chromium (VI) and the amount of chromium (VI) removed by stem cactus were calculated as follows:

$$Removal\ efficiency(\%) = \frac{Co-Ce}{Co} * 100\ldots\ldots\ldots\ldots\ldots\ldots.6$$

Where: Co and Ce= the initial and final adsorbate concentrations

$$qe = \frac{Co-Ce}{Mo} * V\ldots\ldots\ldots\ldots7$$

Where: qe = an adsorption capacity (mg/g), V= the volume of the whole solutions (L) and Mo= mass in gram of test portion of an adsorbent.

The Freundlich and Langmuir equations were used to explain the Cr (VI) removal adsorption equilibrium. Thus, among the several isotherms that could exist, the Langmuir isotherm with the following equation.

$$\frac{Ce}{q} = \frac{1}{qmax} + \frac{1}{nlogCe}\ldots\ldots\ldots\ldots\ldots\ldots\ldots.8$$

The constant b and $q_{max}$ were calculated from the slope and intercept of the graph for each parameter and Freundlich isotherm models was tested by using an equation:

$$Logqe = Logkf + \frac{1}{nlogCe}.....................9$$

Where the slope and intercept of the graph's linear plots were used to compute kf and n. After the data was examined in an Excel sheet, the general equation that produced the best fit.

*c. Data Analysis*

All the resulted data were entered into a Micro soft Excel spread sheet. Then after, the imported data were filtered, checked, effectively coded, and analyzed using a Microsoft Excel (2010), then transferred into R-software (version 4.4.3 (2025-02-28)) and Origin (2022) for further analysis. The hexavalent chromium removal efficacy of both the stem cactus and the commercial activated carbon were evaluated under varying experimental conditions (adsorbent dose, concentration, contact time, pH and stirring speed). The trends in removal efficiency were examined descriptively using line graph. Furthermore, the adsorption equilibrium isotherms (Langmuir and Freundlich) and kinetics models including pseudo-first-order and pseudo-second-order models were fitted to the data to evaluate the biosorption mechanisms and compare the sorption capabilities of the two biosorbents (SC and CAC). Finally, the results were presented by tables, and graphs.

## 3. Results

*a. Adsorbent Characterization*

The moisture, ash, and the volatile contents of the commercial activated carbon (%) were 0.96±0.0.3, 8.31±0.24, and18.45±0. 49, respectively, whereas the stem cactus activated carbon exhibited values of 0.27±0.02, 6.34±0.19, and 27.00±0.82. Furthermore, the bulk density (g/ml), carbon content (%), and the particle size(mm) of the commercial activated carbon were 0.66±0.0.02, 72.28±0.23, and 0.425, respectively, compared to 0.53±0.04, 66.39±0.42, and 0.425 for the stem cactus activated carbon (Table 1).

**Table 1.** Physicochemical characteristics of the commercial activated carbon and activated carbon obtained from cactus stem.

| S/N | Characteristics to be tested | Unit | CAC | RSC | SCAC |
|---|---|---|---|---|---|
| 1 | Moisture content | % | 0.96±0.0.3 | 0.64±0.03 | 0.27±0.02 |
| 2 | Ash content | % | 8.31±0.24 | 8.41±0.2 | 6.34±0.19 |
| 3 | Volatile content | % | 18.45±0.49 | 30.81±0.43 | 27.00±0.82 |
| 4 | Bulk density | g/ml | 0.66±0.0.02 | 0.65±0.02 | 0.53±0.04 |
| 5 | Carbon content | % | 72.28±0.23 | 60.14±0.22 | 66.39±0.42 |
| 6 | Particle size | Mm | 0.425 | 0.425 | 0.425 |

The pH of zero charge (pHpzc) value of more than 3 for the stem cactus-based adsorbent is significantly indicating its adsorption characteristics (Figure 1).

Preprints.org (www.preprints.org) | NOT PEER-REVIEWED | Posted: 31 March 2026 doi:10.20944/preprints202603.2409.v1



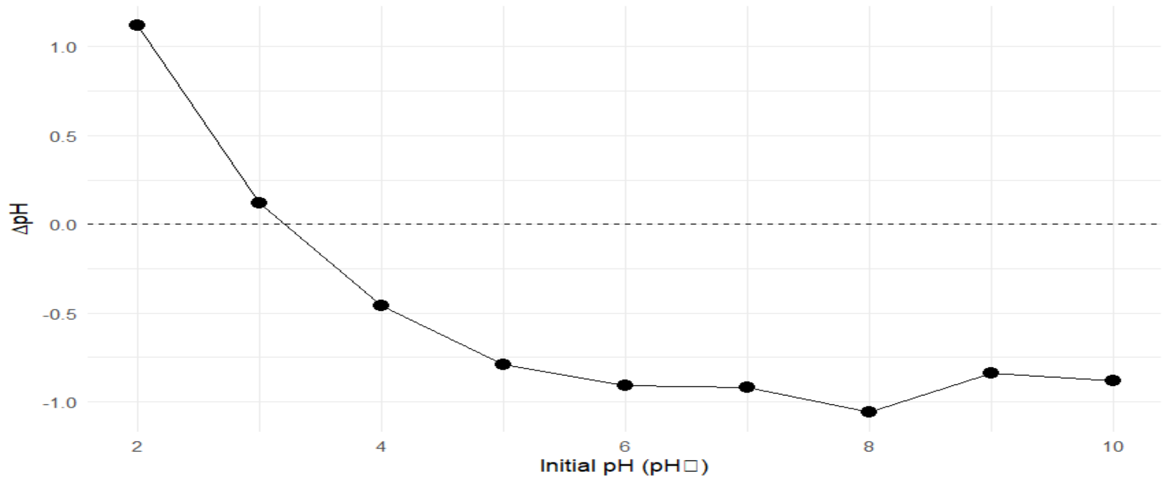


**Figure 1.** Determination of the point of zero charge(pHpzc) of stem cactus adsorbent.

The FTIR spectrum of an adsorbent originated from stem cactus is indicated in Figure2, and exhibited spectral bands ranging from 4000 to 550 $cm^{-1}$ before and after the adsorption processes.

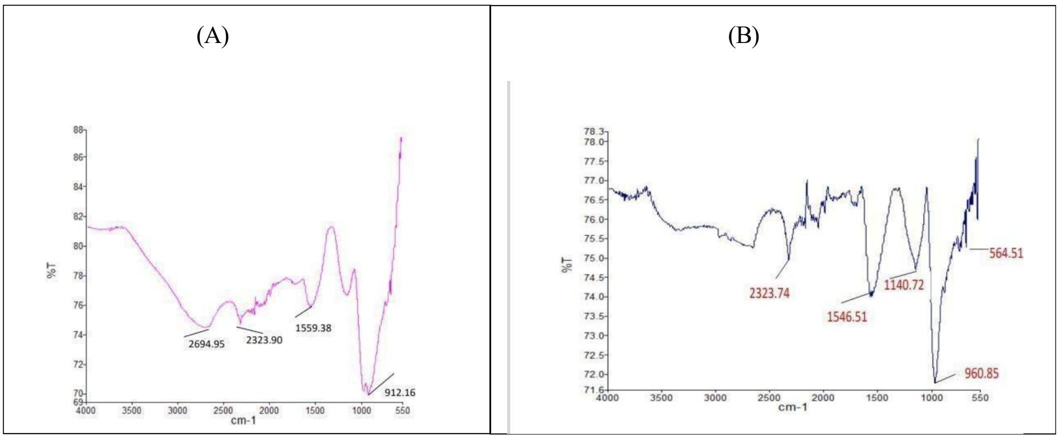


**Figure 2.** FT-IR spectra of stem cactus-based adsorbent before (A) and after hexavalent Chromium loaded (B).

The functional groups which play a significant role in the removal of hexavalent Chromium found in the stem cactus-based adsorbent are presented in Table3 were hydroxyl, aromatics, aromatic and amine, and carboxyl groups.

**Table 2.** The Identified functional groups found in the surface of an activated stem cactus and their corresponding frequencies before and after adsorption processes.

| FTIR-peaks | Frequency before adsorption ($cm^{-1}$) | Frequency after adsorption ($cm^{-1}$) | Difference | Bond type | Functional group |
|---|---|---|---|---|---|
| 1 | 2694.95 | 2323.74 | 371.21 | O-H stretching | Hydroxyl |
| 2 | 2323.90 | 1546.51 | 777.39 | C ≡C stretching | Aromatic (Alkyne) |
| 3 | 1559.38 | 1140.72 | 418.66 | C=C and N-H | Aromatic and Amine |

Preprints.org (www.preprints.org) | NOT PEER-REVIEWED | Posted: 31 March 2026 doi:10.20944/preprints202603.2409.v1



| | | | | | |
|---|---|---|---|---|---|
| | | | | stretching | |
| 4 | 912.16 | 960.85 | -48.69 | C-O, stretching | Carboxyl |

The XRD pattern of the stem cactus-based activated carbon (SCAC) is shown in Figure 3. A wide diffraction peak presented between 2θ = 20°-30º.

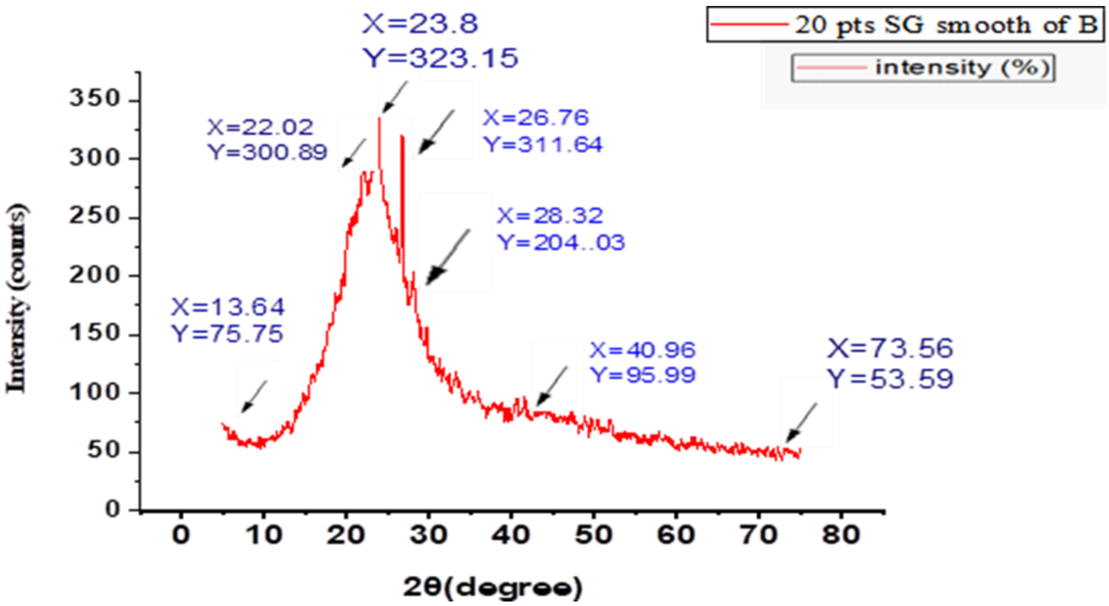


**Figure 3.** XRD patterns stem Cactus-based adsorbent.

The SEM result of the surface stem Cactus- based activated carbon was found to be uneven with troughs and covered in numerous pores, a result of modifications by activating agents or chemicals. SEM images taken at different magnifications power revealed an amorphous morphology. Figure 4 indicates the porous nature of the cactus stem, where irregular and amorphous pores become visible at higher magnifications. Other observed morphologies included spiral tube structures and voids.

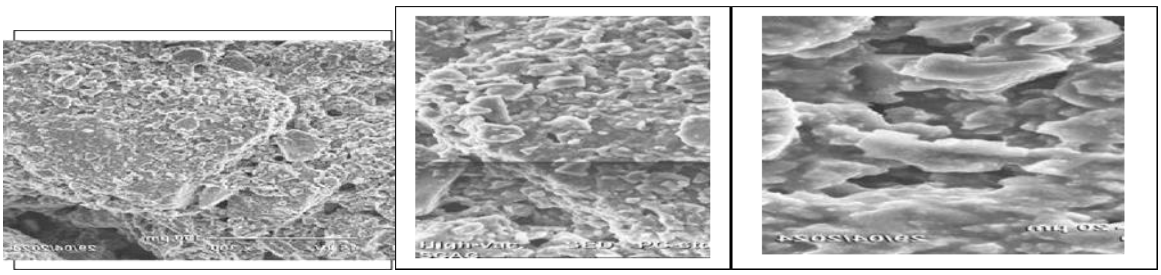

(A)100 μm (B) 50μm (C) 20μm

**Figure 4.** SEM showing surface porosity of an adsorbent.

*b. Batch Adsorption Experiment Result*

i. Effect of Adsorbent on Removal Efficiency

In both stem cactus and commercial activated carbon adsorbents, hexavalent Chromium removal increased with increasing an adsorbent dose. When the initial doses of stem Cactus increased, Cr (VI) removal increased from 89.1% to 98.4%. Among the tested doses of stem cactus

Preprints.org (www.preprints.org) | NOT PEER-REVIEWED | Posted: 31 March 2026 doi:10.20944/preprints202603.2409.v1



adsorbents, 0.15 g was found to be the most effective dose in removing the hexavalent Chromium (93.8%) with a constant concentration at 6mg/l, pH of 2, and contact time of 60 minutes, indicating the equilibrium condition (Figure 5). Comparably, under optimal conditions, commercial activated carbon (CAC) achieved a removal effectiveness of 99.2%. While increasing the dose of an adsorbent from 0.075-1.0g, amount of uptake of metals per unit of gram was slightly decreased from higher to lower (3.564 to 0.295 mg/g).

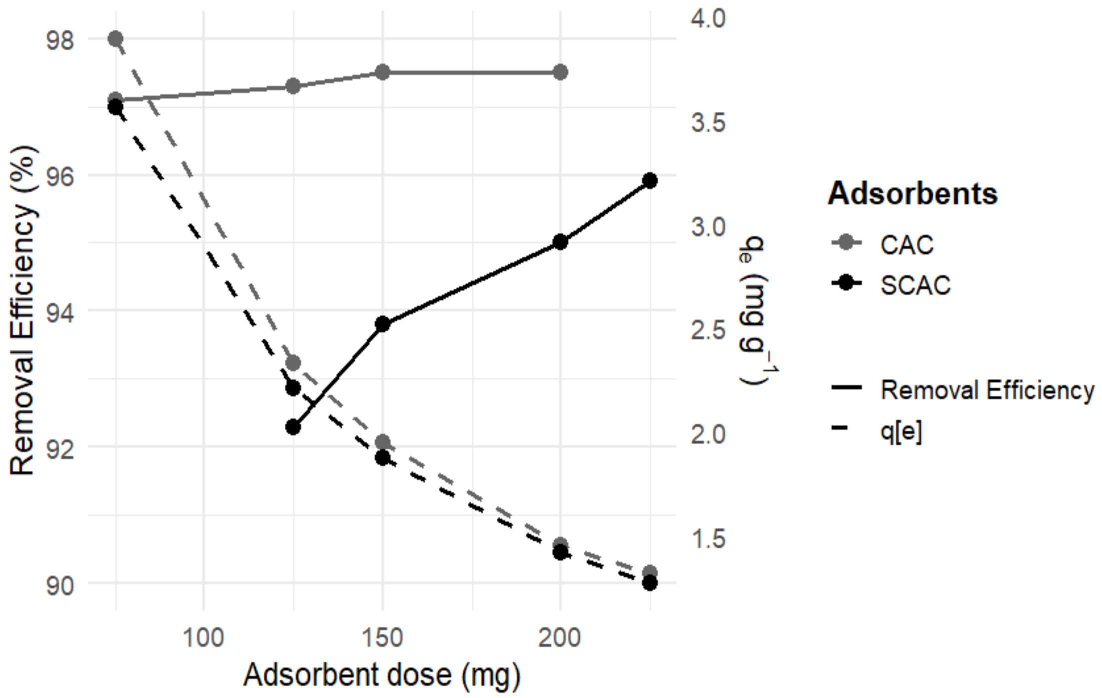


**Figure 5.** Effect of an adsorbents dose on adsorption Performance.

ii. Effect of Initial Concentration of an Adsorbent on Adsorption

In the adsorption experiment, increasing the initial concentrations from 2 to 10 mg/L, Cr (VI) removal efficiencies decreased from 98.0% to 94.6%, while a low (6 mg/L) tested concentration achieved 97.5% removal. Under similar optimal conditions (pH, contact time, shaking speed), commercial activated carbon achieved a few decreasing removal efficiencies from 98.2% to 96.4%, with metal uptake per gram varying from 0.054 to 3.153 mg/g (Figure 6).

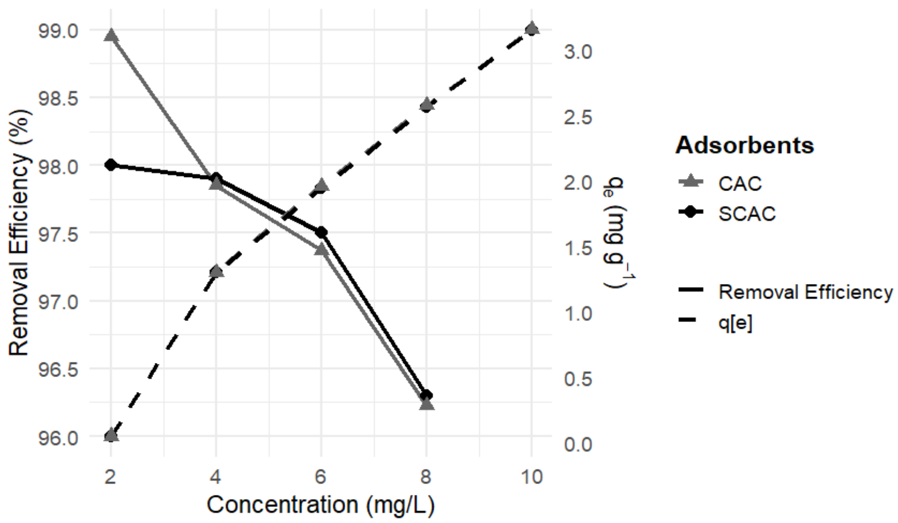

 doi:10.20944/preprints202603.2409.v1



**Figure 6.** The effect of initial concentrations of adsorbents (SCAC vs CAC) on adsorption efficiency.

iii. The Effect of pH

Adsorption experiments were conducted across six different pH levels (2–7) to assess the impact of pH on Cr (VI) removal, and the results indicated that removal efficiency increased with decreasing pH.

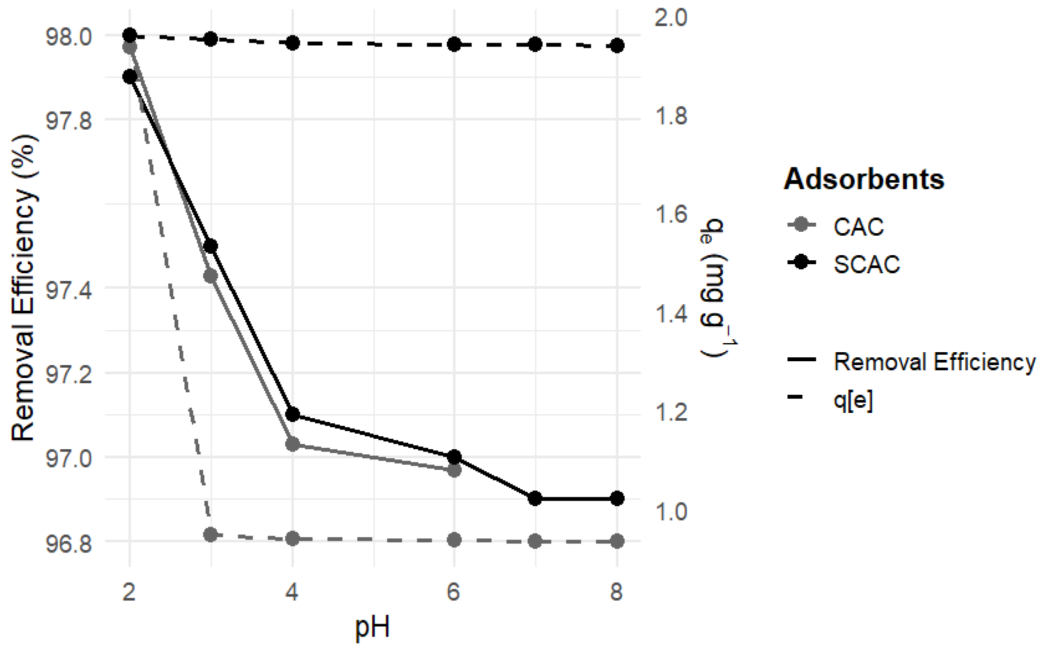


**Figure 7.** Effect of pH on Cr (VI) removal performance (SCAC vs CAC).

iv. The Effect of Contact Time

The effect of contact time duration (30–150 minutes) on the Chromium (VI) removal was evaluated under optimum conditions. The results indicated that increasing duration from 30 to 150 minutes the removal efficiency increased from 94.5 to 98.1% (Figure 8).

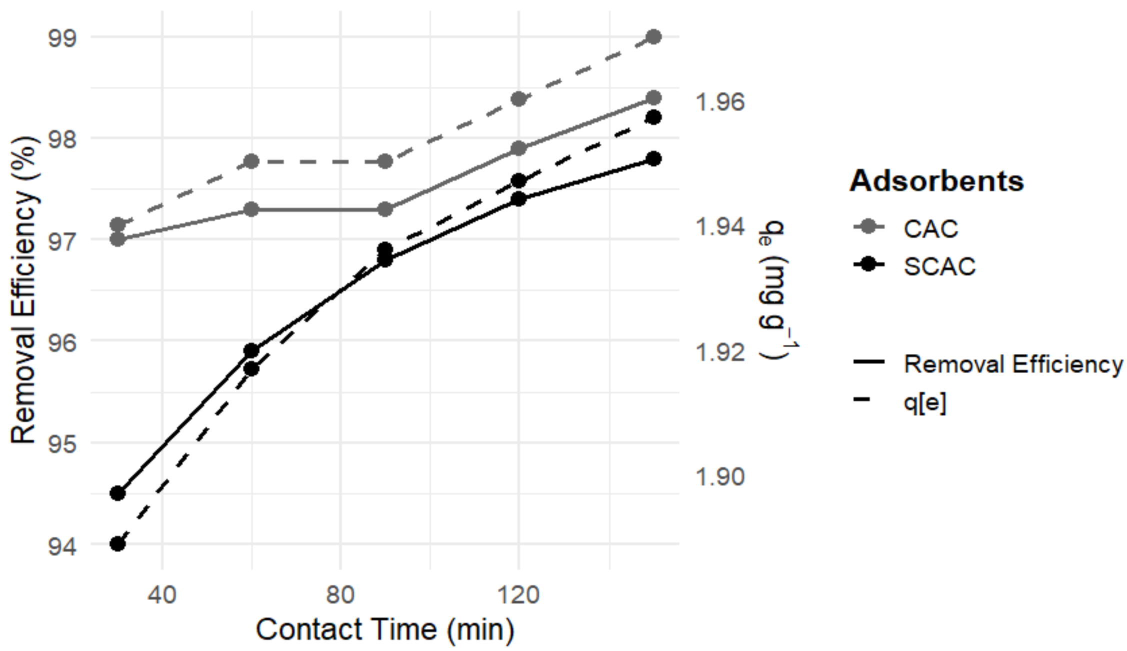

**Figure 8.** Effect of time duration on Cr (VI).

v. The Effect of Shaking Speed and Temperature

The influence of stirring speed on the adsorption of Cr (VI) was evaluated over the range of 50–300 rpm. As the shaking speed increased from 50-300 rpm, removal efficiency progressively increased (Figure 9).

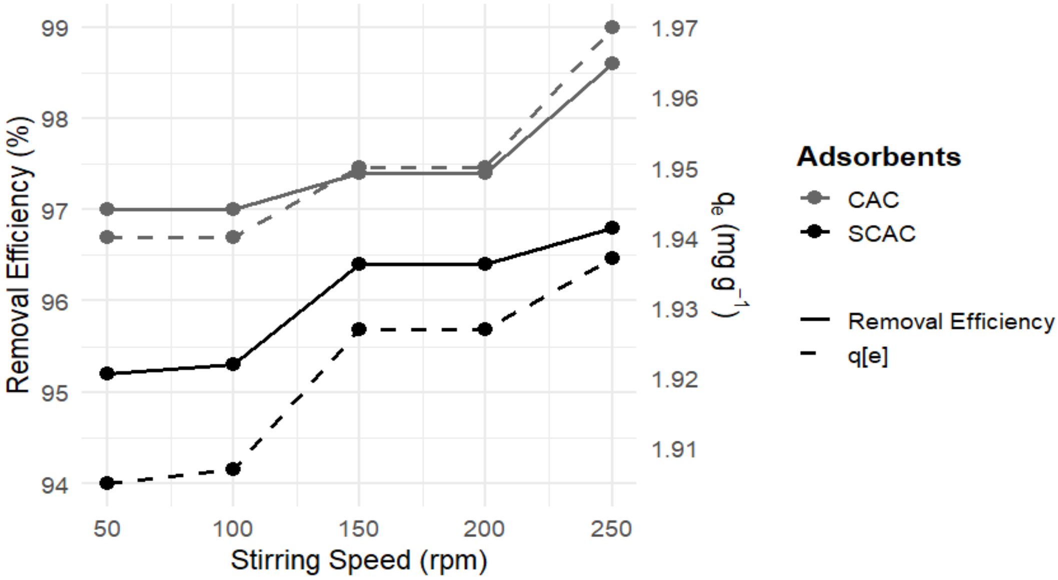


**Figure 9.** Effect of stirring speed on Cr (VI) removal (Adsorption).

*c. Adsorption Isotherm Studies*

i. Langmuir Isotherm Model

The Langmuir isotherm model for Cr (VI) ion adsorption onto the SCAC and CAC is shown in Figure 10. The slope and the intercept of the linear regression were $1/q_{max}$ and $1/(q_{max}b)$, respectively. The Langmuir constant was calculated from the regression equation. The $q_{max}$ (The maximum adsorption) and b (The Langmuir constant related to energy of adsorption) were determined to be 4.23 mg/L and 5.37mg/g, respectively, which indicates the affinity of the SCAC and CAC toward Cr (VI) ion. The correlation coefficient ($R^2$) of CAC and SCAC were 0.9994 and 0.9985, respectively, suggesting the suitability of this model for illustrating the equilibrium adsorption process.

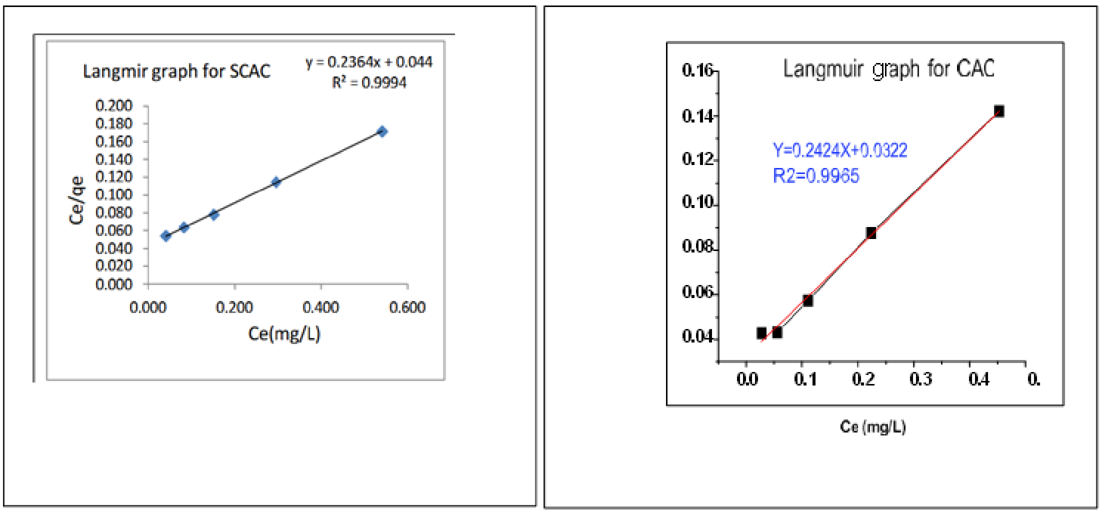

Preprints.org (www.preprints.org) | NOT PEER-REVIEWED | Posted: 31 March 2026 doi:10.20944/preprints202603.2409.v1



**Figure 10.** Langmuir isotherm graph for Chromium ion removal onto Cactus stem and commercial activated carbon.

The $R_L$ value was determined using Langmuir constant and the initial Cr (VI) ion concentration. The $R_L$ of this study was ranged from 0.02309-0.1057 (Figure 11), indicating suitable condition for Cr (VI) ion adsorption onto the adsorbent.

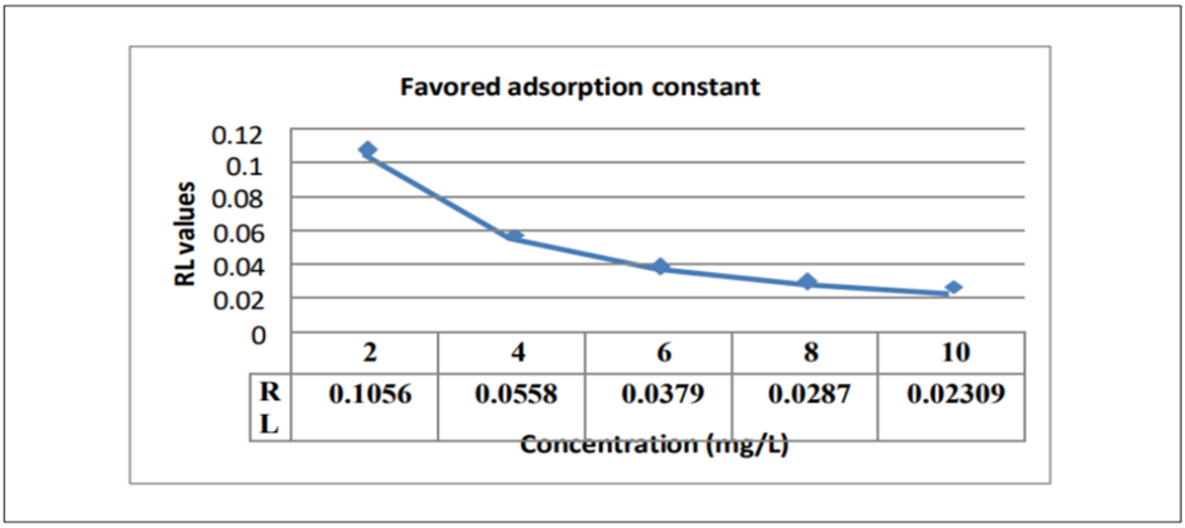


**Figure 11.** Langmuir separation factor with different initial concentrations.

ii. Freundlich Isotherm Model Analysis

Cr (VI) ion adsorption onto SCAC and CAC based on Freundlich isotherm model is indicated in Figure 12. This model was applied to illustrate the adsorption properties of Cr (VI) onto the adsorbents, by plotting $\log_{qe}$ vs $\log_{Ce}$, which produced a straight-line revealed that the adsorption experiment followed the Freundlich model. The adsorption capacity constants were determined from the intercept and slope of the linear regression graph (Figure 12). The Kf and 1/n values obtained to 5.15 and 0.594, respectively. The high correlation coefficients of SCAC and CAC (R2=0.9385 and 0.9256, respectively), suggesting a good fit for adsorption occurs on a heterogenous surface with multilayer formation.

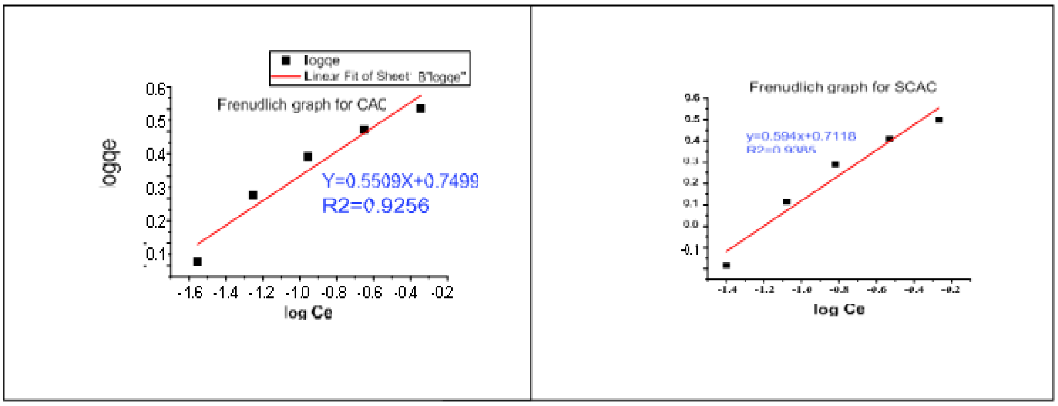


**Figure 12.** Freundlich isotherm graph for Cr (VI) adsorption onto the adsorbents.

*d. Kinetics of SCAC and CAC Mediated Cr (VI) Removal Adsorption*

a) Pseudo first order kinetics model

Figure 13 presents the pseudo first order kinetic model for the adsorption of Cr (VI) ion onto the surface of the adsorbents. The linear plot of log (qe-qt) against time was used to calculate $K_1$(the rate constant) and $q_e$ (the equilibrium adsorption capacity) from the slope and the intercept, respectively. In this investigation, the calculated equilibrium adsorption capacity value (0.1812 mg/g) was significantly smaller than the experimental value (1.95) and qe (calculated=0.1812), indicating that the pseudo first order kinetics model did not properly describe the adsorption behavior of Cr (VI) ion onto the surface of the adsorbents (SCAC and CAC).

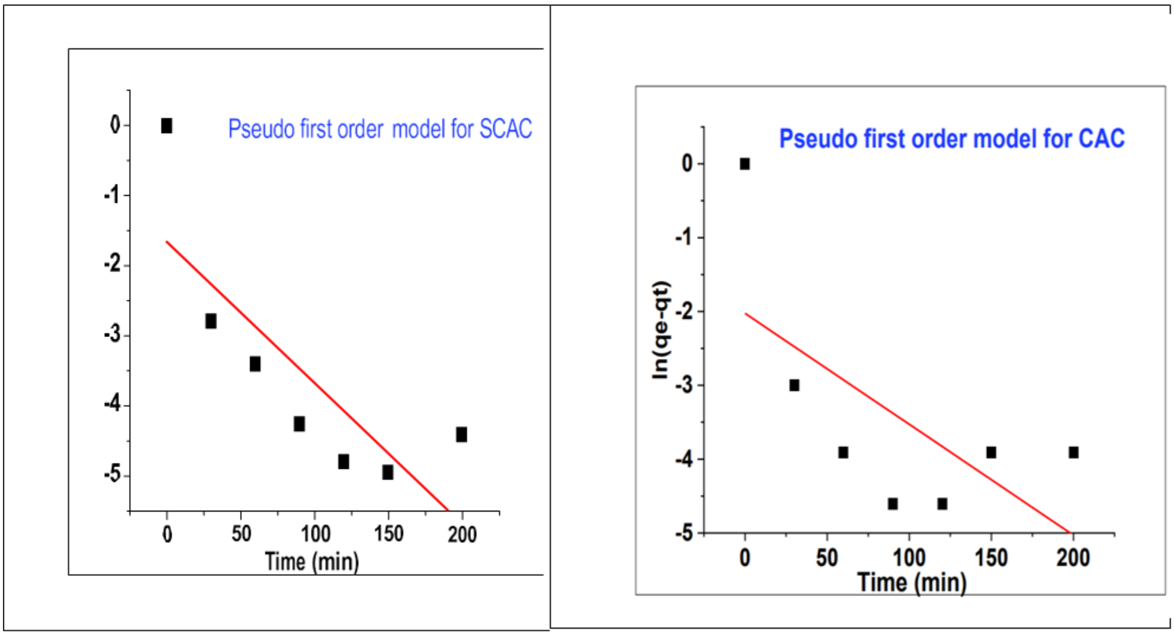


**Figure 13.** Pseudo first order kinetics model for Cr (VI) adsorption.

b) Pseudo second order kinetics model

The pseudo second order kinetic model for the adsorption of Cr (VI) onto the surface of the adsorbents is presented in Figure 14. The linear plot t/qt versus t revealed a strong linear relationship, indicating that the adsorption process respects the pseudo second order kinetics model. The correlation coefficient ($R^2$) for both SCAC and CAC were 0.99992 and 0.99991, respectively, suggesting a good fit for adsorption process.

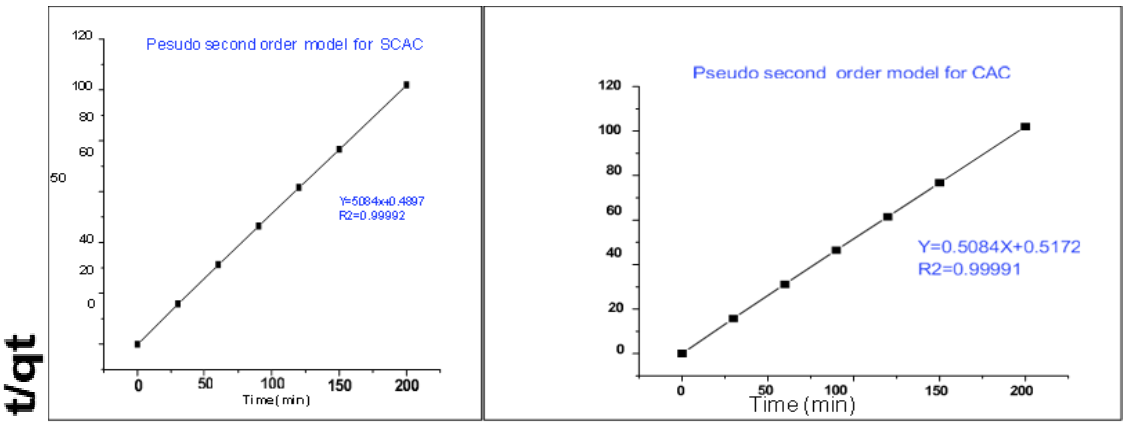


**Figure 14.** Pseudo second order kinetics for SCAC and CAC mediated Cr (VI) removal.

*e. Removal of Chromium (VI) from Wastewater Using Stem Cactus Adsorbent*

The bio sorbent was able to effectively removal Cr (VI) from the actual tannery waste water. Tests were conducted based on previously optimized study setting. The removal efficiency of Chromium by stem cactus activated was progressively increased with increasing contact time (Figure

Preprints.org (www.preprints.org) | NOT PEER-REVIEWED | Posted: 31 March 2026 doi:10.20944/preprints202603.2409.v1



15). Under the optimized conditions (pH of 2.0, an adsorbent dose of 0.15g, and at room temperature), removal efficiency increased with contact time. Unlike the normal solution, which accomplished its maximum removal efficiency at 60 minutes, the optimized condition reached an adsorption efficiency of 89.25% ± 0.23% at 90 minutes. Further increases beyond this point did not yield a significantly improvement in the adsorption efficiency. Furthermore, the rate of Chromium adsorption using stem cactus activated carbon was comparable to the finding that observed in the batch experiment conducted using a standard solution, both in early and final stages under the adjusted conditions.

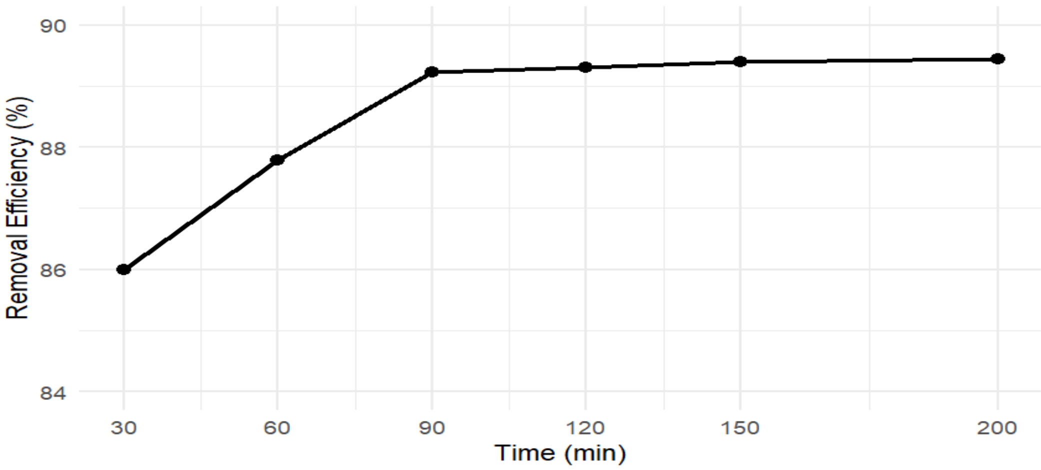


**Figure 15.** The effect of contact time on Cr (VI) removal from real wastewater under the optimum conditions of pH, adsorbent dose, and Temperature.

## 4. Discussion

The characterization results showed that the activated carbon derived from stem cactus (SCAC) exhibited significantly lower moisture content (0.27%) than the commercial activated carbon (0.96%). This indicated that the stem cactus has more active sites for the adsorbate (Cr(VI) to promote the adsorption process(Zhou et al., 2001). Activated carbon obtained from stem cactus characterized by a higher volatile content (27.00±0.82%) than the commercial activated carbon (18.45±0.49%). This revealed that maximum portion of the adsorbent lost as gas and liquid , which can affect the fixed carbon yield and critically affect surface structure properties and pore size, which is important for adsorption process(Chakraborty et al., 2025) .Its bulk density (0.53±0.04 g/mL) was a little bit lower than the commercial one (0.66±0.0.02 g/mL) suggested that the stem cactus adsorbent has high porosity, which promotes adsorption process (Liu et al., 2018). The activated carbon obtained from stem cactus processing exhibited a lower carbon content (66.39±0.42%) than the commercial activated carbon, which contained 72.28±0.23% of carbon (table-1) indicates its lower carbonaceous structure, which reduced adsorption capacity due to lower surface area and active sites (Sabzehmeidani et al., 2021).

The pHpzc value (greater than 3) of the present adsorbent (stem cactus -based adsorbent) is slightly lower than those reported by (4.96; Kumar et al., 2025), indicating its greater adsorption efficiency. When the solution pH is exceeded the pHpzc, the functional groups found lose its hydrogen ion ($H^+$), and the surface charge changed to anion. This phenomenon is consistent with the present observation. Whereas, when the solution pH values smaller than the pHpzc, the surface charge changed to positive, promoting biosorption of anionic pollutant (Malima et al., 2021).

The FTIR spectra of stem cactus before and after Cr (VI) adsorption are indicated in Table 3. The spectrum showed different characteristic peaks corresponding to the bond type and functional groups such hydroxyl, aromatic (alkyne), aromatic and amine and carboxyl groups. A noticeable shift of -48.69 was observed for the bond associated with the carboxyl group, indicating its participation in Cr (VI) binding. Large differences showed in some peaks may be due to change in the surface molecular arrangements of the adsorbent after Cr (VI) adsorption, indicating that possible interaction between Cr (VI) ion and the functional group of the adsorbent (Gupta et al., 2015; Kamilia et al., 2025).

The XRD broad pattern presented in Figure 3, indicating that the primary appearance of an amorphous carbon structure with inadequate long-range of crystalline structure, this attribute suggesting that mainly non-crystalline nature of the material at 323.15 K. On the other hand, absence of sharp peak associated to crystalline impurity indicating that the activation process did not add significant crystalline phase, and the adsorbent's structure dominated by amorphous carbon characterized by high porosity and disorder carbon frameworks, which provide accessible adsorption sites to promote the transfer of a pollutant into the pore (Zerin et al., 2025).

The SER analysis provided perceptions into surface morphology of the stem cactus. It exhibited different morphology. The high porous and uneven surface promotes adsorption process by providing a number of accessible sites, and as it promotes surface area. This is in agreement with studies other studies for different bio-based carbon, which have improved adsorption capacity by increasing the transfer and diffusion of a pollutant (Sabzehmeidani et al., 2021).

The effect of adsorbent dose on Cr (VI) removal is presented in Figure 5. The result showed that adsorbent dose significantly influences Cr (VI) removal. When the initial doses of stem cactus increased, Cr (VI) removal increased from 89.1% to 98.4%. Increasing the dose of an adsorbent promote the surface-active site of the biosorbent material and the available specific surface area, which enhance adsorption process, and consequently the removal of the Cr (VI) will increase (Khalifa et al., 2019).

The initial concentration of Cr (VI) concentration on adsorption efficiency is shown in Figure 6. As the initial Cr (VI) ion concentration increased concentrations from 2 to 10 mg/L, Cr (VI) removal efficiencies decreased from 98.0% to 94.6%. This indicates that there are fewer available active sites per Cr (VI) ion on the surface of the SCAC as concentration increases. Consequently, the percentage of removal may decline as the initial concentration increased because higher dose of adsorbent provides maximum number of active sites, and surface area, which promote interaction between the Cr (VI) and the adsorbent. However, at higher dose, the adsorbent particles can combine together and reduced available surface area and active site for adsorption process. High adsorbent dose can cause poor dispersion, reduce the effective contact between the adsorbent and the adsorbate (Wongjunda & Saueprasearsit, 2010).

The pH of the solution significantly influences the adsorption performance. The highest removal efficiency (98.48%) achieved within a pH range of 2–3 (Figure 7), indicating that pH 2 is the optimum pH for maximum Cr (VI) removal. As the pH increases, the surface of the adsorbent becomes more negatively charged. This creates a repulsion between the adsorbent and the adsorbate. Therefore, Chromium removal efficiency decreases as the pH increases (Padmavathy et al., 2016).

The adsorption of Cr (VI) ion onto stem cactus adsorbent was time-dependent process, with a rapid increase in removal efficiency from 94.5 to 98.1% during from 30-150 minutes (Figure 8). Maximum removal of efficiency was achieved at 60 minutes, indicating the optimal contact time for achieving maximum removal efficiency. However, further increasing the duration from 60 minutes to 200 minutes did not yield a significant Chromium removal because the adsorbent surface coverage is high, and all the accessible adsorbent surface is already saturated (Padmavathy et al., 2016; (Khalifa et al., 2019).

The efficiency of Cr (VI) using stem cactus adsorbent was dependent on stirring speed. The adsorption efficiency was increased progressively from 97.65% to 98.8% with increasing stirring speed. This finding is consistent with other study reported by Chen et al. (2012), who documented that quick stirring speed results maximum adsorption efficiency. The effect of temperature on hexavalent Chromium removal efficiency was examined over a range of 25-35 °C. Among the tested temperature, 25 °C found to be the most favorable condition for 98.4% of Cr (IV) removal. As the initial temperature of the solution increases, the adsorption process also increases, indicating that adsorption is an endothermic process. This finding is the same as the findings of Cr(III) adsorption using bentonite clay by (Tahir & Naseem, 2007).

The good fit of the Langmuir isotherm model to the adsorption data, as indicated in Figure 10 and the $q_{max}$ (The maximum adsorption) and b (The Langmuir constant related to energy of adsorption) 4.23 mg/L and 5.37mg/g, respectively, indicating a monolayer adsorption of Cr (VI) ion. This suggests a homogenous surface involving finite number of identical adsorption sites. The Langmuir isotherm model posits that adsorption happens as monolayer on a consistent and uniform adsorbent surface. It depends upon the principle that inadequate number of specific adsorption sites that occur with each site capable of adsorbing solitary a single molecule or ions (Kumar et al., 2025). The $R^L$ value of this study was ranged from 0.02309-0.1057 (Figure 11), indicating a more favorable condition for Chromium removal. The most widely used and scientifically confirmed $R^L$ value for the adsorption process to be favorable falls between 0 and 1(Hall et al., 1966).

The Freundlich isotherm model offered an excellent fit for the adsorption data, with a correlation coefficient for SCAC and CAC $R^2$=0.9386 and 0.9256, respectively, indicating that Cr (VI) adsorption happens on the heterogenous surfaces, and the chance of multilayer adsorption. The adsorption capacity (Kf)and intensity (1/n) were determined from the intercept and slope of the linear regression graph (Figure 12), respectively. The Kf and 1/n values obtained to 5.15 and 0.594, respectively, indicating favorable adsorption, and heterogeneous surface characterized by a non-identical adsorption site and a strong adsorption affinity of Chromium ion onto the adsorbent. Unlike the Langmuir model, the Freundlich suggests that, the adsorption process operates at different sites, leading to the probability of multiple biosorption. This model suggests that adsorption process contrasts across different surface sites (Sheeja et al., 2021).

The pseudo first order kinetics model was employed to assess the adsorption mechanism of Cr (VI) ion onto the adsorbents. In this investigation, the calculated equilibrium adsorption capacity value (0.1812 mg/g) was significantly smaller than the experimental value (1.95) and qe (calculated=0.1812), indicating that the pseudo first order kinetics model did not properly describe the adsorption behavior of Cr (VI) ion onto the surface of the adsorbents (SCAC and CAC). In the adsorption process, pseudo first order kinetics describes the kinetics at the early stage of the process. The model was evaluated to illustrate the adsorption of Cr (VI) onto the adsorbents (Both the cactus stem and the commercial activated carbon) (Ho & McKay, 1999). The pseudo second order kinetics model indicated a better agreement with the experimental adsorption data than the pseudo first order kinetics model, as confirmed by the highest correlation coefficients. From Figure 13, the correlation coefficient ($R^2$) for both SCAC and CAC were 0.99992 and 0.99991, respectively, suggesting that the SCAC and CAC mediated Cr(VI) removal was best described by the pseudo second order reaction (Choudhary & Paul, 2018).

The rapid observed increase in adsorption efficiency during the initial stage may be attributed to the presence of greater number of surface-active sites. The increase in removal efficiency within contact time under the optimized conditions (pH, temperature and dose of an adsorbent) shows that Cr (VI) ion removal by stem cactus activated carbon-mediated adsorption is a time-dependent process. The delayed achievement of adsorption efficiency at 90 minutes, compared with 60 minutes for the normal solution, indicates that the optimized conditions affect the sorption of the pollutant. The adsorption performance of stem cactus activated carbon was further tested using a real wastewater sample collected from Awash leather factory, which had an initial hexavalent Chromium ion concentration of 1.03±0.05mg/L. Under the optimum conditions, the adsorption efficiency of 89.25%±0.23% was achieved. However, this adsorption efficiency was slightly less than that of the standard solution, the variation can be attributed to the existence of additional metals and pollutants in the actual wastewater that interfere or compete with adsorption efficiency. Furthermore, adsorbent fouling and surface passivation, complexity of matrix effects are the factors that influence removal efficiency. In spite of the reduced efficacy compared with the synthetic solution, the attained Chromium removal remains effective for practical application. Adsorption efficiencies more than 80% are generally practically acceptable for heavy metal treatment, particularly environmentally friendly treatments (natural adsorbents) (Fu & Wang, 2011).

However, this study did not carry out additional research to investigate the chromium (VI) removal efficiency of stem cactus powder by continuous filling of the biosorbent in successive columns. The present study did not study the thermodynamics parameters [entropy ΔS), gibes free energies ΔG, and enthalpy ΔH]. Studies on SCAC adsorptive efficiency with other necessary ions or trace elements may not be assessed.

## 5. Conclusions

This study indicated that plant-based adsorbents have a substantial potential for the effective removal of hexavalent Chromium from both real wastewater and synthetic wastewater. For this experiment, stem cactus used as an adsorbent, and was activated using locally available chemical ($H_3PO_4$) to increase Cr (VI) removal. The physicochemical compositions of the adsorbent such as moisture content, ash content, volatile matter, point of zero charge, surface functional groups were characterized. Then, the Cr (VI) removal performance of the adsorbents (both stem cactus activated carbon and commercial activated carbon) under different conditions (pH, temperature, dosage of adsorbents, stirring speed and contact time) were evaluated. Cr (VI) adsorption is highly pH dependent process. In conclusion, under optimized condition (pH of 2, an initial concentration of 6 mg/L, adsorbent dose of 150g, a shaking speed of 200 rpm, a duration of 60 minutes, and at room temperature), stem cactus adsorbent and commercial activated carbon achieved Cr (VI) removal of 98.4% and 99.2%, respectively, indicating that the prepared stem cactus-based adsorbent had a comparable Cr (VI) removal efficiency with the commercial activated carbon. The adsorption performance of stem cactus activated carbon was further tested using a real wastewater sample that contain a concentration of 1.03±0.05mg/L Cr (VI) ion collected from Awash leather factory. Under the optimum conditions, the adsorption efficiency of 89.25%±0.23% was achieved. The adsorption data indicates that both the Freundlich and Langmuir isotherm models are the best fitting models. The adsorption process is an endothermic process and respects the pseudo second order kinetics model. The present study suggests that plant-based adsorbents represent an effective choice for heavy metal removal to replace expensive adsorbents such as commercial activated carbon.

**Authors contribution: Destaw Sitotaw:** Conceptualization, Data curation, Formal Analysis, Investigation, and Writing-original draft**. Tesfaye Ababu:** Conceptualization, Analysis, Supervision, review and editing. **Andualem Mekonnen**: Conceptualization, Analysis, Supervision, provision of resources, and reviewing and editing. **Tadesse Alemu**: Analysis, supervision, and reviewing and editing.

**Funding statement:** This investigation did not receive any specific fund from any grants or funders.

**Data availability statement:** Data will be made available on request.

**Statement of Declaration of interest:** The authors declared that they have no competing or conflict of interests.

## References

Alfarra, R. S., Ali, N. E., &, & Mashita Mohd Yusoff, M. M. Y. (2014). Removal of Heavy Metals by Natural Adsorbent: Review. *International Journal of Biosciences (IJB)*, *4*(7), 130–139.

AOAC, A. of O. A. C. (2000). *Official methods of analysis of the Association of Official Analytical Chemists* (W. Horwitz (ed.); 17th Editi). AOAC Internationaln.

APHA. (1926). *Standard methods for the examination of water and wastewater* (Association (ed.); 6th ed.). American Public Health Association (APHA).

Chakraborty, S., Aktay, N., Alptekin, F. M., Celiktas, M. S., & Dunford, N. T. (2025). Effect of Process Parameters and Biomass Type on Properties of Carbon Produced by Pyrolysis. *Biomass*, *5*(3), 52.

Chen, Y. G., He, Y., Ye, W. M., Lin, C. H., Zhang, X. F., & Ye, B. (2012). Removal of chromium(III) from aqueous solutions by adsorption on bentonite from Gaomiaozi, China. *Environmental Earth Sciences*, *67*(5), 1261-1268. https://doi.org/10.1007/s12665-012-1569-3

Choudhary, B., & Paul, D. (2018). Isotherms, kinetics and thermodynamics of hexavalent chromium removal using biochar. *Journal of Environmental Chemical Engineering*, *6*(2), 2335–2343. https://doi.org/10.1016/j.jece.2018.03.028

Clesceri, L. S., Greenberg, A. E., & Eaton, A. D. (1998). *Standard Methods for the Examination of Water and Wastewater* (A. D. Clesceri, L. S., Greenberg, A. E., & Eaton (ed.); 20th ed.). American Public Health Association.

Derbe, T., & Yilma, B. (2015). Spectroscopic investigation of metal level in Aloe Vera plant , and the soil where the Aloe Vera grows : Arba Minch , southern Ethiopia. *Modern Chemistry*, *3*(1), 1–8. https://doi.org/10.11648/j.mc.20150301.11

DesMarias, T. L., & Costa, M. (2019). Mechanisms of chromium-induced toxicity. *Current Opinion in Toxicology*, *14*, 1–7. https://doi.org/10.1016/j.cotox.2019.05.003

Duran-valle, C. J. (1999). Formation of oxygen structures by air activation . A study by FT-IR spectroscopy. *Carbon*, *37*(10), 1517–1528.

Edo, G. I., Itoje-akpokiniovo, L. O., Obasohan, P., Ikpekoro, V. O., Samuel, P. O., Jikah, A. N., & Agbo, J. J. (2024). Impact of environmental pollution from human activities on water, air quality and climate change. *Ecological Frontiers*, *44*(5), 874–889.

Eghonghon, K., Osagie, U., Birundu, R., Nwankwo, W., Adelaja, O., Kamdem, H., Monday, O., Oluwaseun, C., & Uzuazor, I. (2021). Effect of hexavalent chromium on the environment and removal techniques : A review. *Journal of Environmental Management*, *280*(September 2020), 111809. https://doi.org/10.1016/j.jenvman.2020.111809

El-araby, H. A., Moneim, A., Ahmed, M., Mangood, A. H., & Abdel-rahman, A. A. (2017). Sesame Husk as Adsorbent for Copper ( II ) Ions Removal from Aqueous Solution. *Ournal of Geoscience and Environment Protection*, *5*(07), 109. https://doi.org/10.4236/gep.2017.57011

Emirie, M. (2015). Removal of chromium hexavalent (Cr(VI) from aqueous solution using activated carbon prepared from Prosopis Juliflora Plant and find the optimal operating condition for adsorption process. Addis Ababa University.

Fu, F., & Wang, Q. (2011). Removal of heavy metal ions from wastewaters: a review. *Journal of Environmental Management*, *92*(3), 407–418. https://doi.org/10.1016/j.jenvman.2010.11.011

Gupta, V. K., Nayak, A., & Agarwal, S. (2015). Bioadsorbents for remediation of heavy metals : Current status and their future prospects. *Environmental Engineering Research*, *20*(1), 1–18.

Hall, K. R., Eagleton, L. C., Acrivos, A., & Vermeulen, T. (1966). Pore-and solid-diffusion kinetics in fixed-bed adsorption under constant-pattern conditions. *Industrial & Engineering Chemistry Fundamentals*, *5*(2), 212-223.

Ho, Y. S., & McKay, G. (1999). Pseudo-second order model for sorption processes. *Process Biochemistry*, *34*(5), 451–465.

Illingworth, J. M., Rand, B., & Williams, P. T. (2012). Novel activated carbon fibre matting from biomass fibre waste. *Proceedings of the Institution of Civil Engineers – Waste and Resource Management*, 123–132.

Islam, M., Mohana, A. A., Rahman, A., Rahman, M., Naidu, R., & Rahman, M. M. (2023). A Comprehensive Review of the Current Progress of Chromium Removal Methods from Aqueous Solution. *Toxics*, *11*(3), 252.

Kamilia, S., Mukhayani, F., Sutarno, S., & Nuryono, N. (2025). Modification of Chitosan-Coated Magnetic Material with Glycidyl-trimethylammonium Chloride for Cr ( VI ) Adsorption. *Indonesian Journal of Chemistry*, *25*(1), 244–255. https://doi.org/10.22146/ijc.100749

Kebede, B. (2013). Assesment of Cactus Potential as a Natural Coagulant in Water Treatment. Addis Ababa University.

Khalifa, E. Ben, Rzig, B., Chakroun, R., Nouagui, H., & Hamrouni, B. (2019). Chemometrics and Intelligent Laboratory Systems Application of response surface methodology for chromium removal by adsorption on low-cost biosorbent. *Chemometrics and Intelligent Laboratory Systems*, *189*(January), 18–26. https://doi.org/10.1016/j.chemolab.2019.03.014

Kumar, M. A., Swarnalatha, A. P., Naveen, K. N., Raju, J. N. S., Kerur, S. S., & Priyadharsini, K. (2025). Biosorption of heavy metals using Plant-Derived Sorbents : An Environmental Solution for Industrial Wastewater. *GLOBAL NEST JOURNAL*, *27*(4).

Liu, J., Liu, X., Sun, Y., Sun, C., Liu, H., Stevens, L. A., & Snape, C. E. (2018). High Density and Super Ultra-Microporous-Activated Carbon Macrospheres with High Volumetric Capacity for CO 2 Capture. *Advanced Sustainable Systems*, *2*(2). https://doi.org/10.1002/adsu.201700115

Malima, N. M., Owonubi, S. J., Lugwisha, E. H., & Mwakaboko, A. S. (2021). Thermodynamic, isothermal and kinetic studies of heavy metals adsorption by chemically modified Tanzanian Malangali kaolin clay. *International Journal of Environmental Science and Technology*, *18*(10), 3153-3168. https://doi.org/10.1007/s13762-020-03078-0

Mane, P., Bhosle, A. S., & Jangam, C. (2011). Heavy Metal Removal from Aqueous Solution by Opuntia : A Natural Polyelectrolyte Heavy Metal Removal from Aqueous Solution by Opuntia : A Natural Polyelectrolyte. January.

Mohammadi, H., Gholami, M., & Rahimi, M. (2009). Application and optimization in chromium-contaminated wastewater treatment of the reverse osmosis technology. *Desalination and Water Treatment*, *9*(1–3), 229–233. https://doi.org/10.5004/dwt.2009.808

Padmavathy, K. S., Madhu, G., & Haseena, P. V. (2016). A study on effects of pH, adsorbent dosage, time, initial concentration and adsorption isotherm study for the removal of hexavalent chromium (Cr (VI)) from wastewater by magnetite nanoparticles. *Procedia Technology*, *24*, 585–594. https://doi.org/10.1016/j.protcy.2016.05.127

Pragathiswaran, C., Sibi, S., & Sivanesan, P. (2013). Adsorption of hexavalent chromium from aqueous solutions by Aloe vera leaf. *International Journal of Research in Pharmacy and Chemistry (IJRPC)*, *3*(4), 876–880.

Preočanin, T., & Kallay, N. (2006). Point of Zero Charge and Surface Charge Density of TiO 2 in Aqueous Electrolyte Solution as Obtained by Potentiometric Mass Titration *. *Croatica Chemica Acta*, *79*(1), 95–106.

Racero-Galaraga, D., Rhenals-Julio, J. D., Sofan-German, S., Mendoza, J. M., & Bula-Silvera, A. (2024). Results in Chemistry Proximate analysis in biomass : Standards , applications and key characteristics. *Results in Chemistry*, *12*(4). https://doi.org/10.1016/j.rechem.2024.101886

Reza, R. A., & Ahmaruzzaman, M. (2015). A novel synthesis of Fe 2 O 3@ activated carbon composite and its exploitation for the elimination of carcinogenic textile dye from an aqueous phase. *Rsc Advances*, *5*(14), 10575–10586.

Sabzehmeidani, M. M., Mahnaee, S., Ghaedi, M., Heidari, H., & Roy, V. A. (2021). Materials Advances for inorganic and organic compounds. *Materials Advances*, *2*(2), 598–627. https://doi.org/10.1039/d0ma00087f

Sheeja, J., Sampath, K., & Kesavasamy, R. (2021). Experimental Investigations on Adsorption of Reactive Toxic Dyes Using Hedyotis umbellate Activated Carbon. *Adsorption Science & Technology*, 12. https://doi.org/10.1155/2021/5035539

Tahir, S. S., & Naseem, R. (2007). Removal of Cr ( III ) from tannery wastewater by adsorption onto bentonite clay. *Separation and Purification Technology*, *53*(3), 312–321. https://doi.org/10.1016/j.seppur.2006.08.008

Uddin, A. N., Burns, F. J., Rossman, T. G., Chen, H., Kluz, T., & Costa, M. (2007). Dietary chromium and nickel enhance UV-carcinogenesis in skin of hairless mice. *Toxicology and Applied Pharmacology*, *221*(3), 329-338.

Vimercati, L., Gatti, M. F., Gagliardi, T., Cuccaro, F., Maria, L. De, Caputi, A., Quarato, M., & Baldassarre, A. (2017). Environmental exposure to arsenic and chromium in an industrial area. *Environmental Science and Pollution Research*, *24*(12), 11528–11535. https://doi.org/10.1007/s11356-017-8827-6

Wongjunda, J., & Saueprasearsit, P. (2010). Biosorption of chromium (VI) using rice husk ash and modified rice husk ash. *Environmental Research Journal*, *4*(3), 224–250.

Zerin, N. H., Rasul, M. G., Jahirul, M. I., Sayem, A. S., Quadir, Z., & Haque, R. (2025). XRD Characterization of Activated Carbons Synthesized from Tyre Pyrolysis Char via KOH Activation. *Technologies*, *13*, 12.

Zhou, L., Li, M., Sun, Y., & Zhou, Y. (2001). Effect of moisture in microporous activated carbon on the adsorption of methane. *Carbon*, *39*(5), 773–776.